

# Attrition milling of metallic-ceramic particles in acetyl-acetone

Ying Yuan, Xin Wang, Ping Xiao\*

*Manchester Materials Science Centre, University of Manchester, Manchester M1 7HS, UK*

Received 10 January 2003; received in revised form 27 July 2003; accepted 29 July 2003

## Abstract

Suspensions were prepared from attrition-milling of a mixture of yttria-stabilised zirconia (YSZ) and aluminium (Al) in acetyl-acetone (ACAC). The attrition milling not only reduced the particle size of the powder mixture, but also reduced the YSZ crystallite size. One factor contributing to reduction in both particle size and crystallite size was chemical reaction between YSZ and ACAC during attrition milling. TEM of the particles before and after milling confirmed the effect of the chemical reaction. Thermal analyses and dilatometer measurements of the green compact made from these particles indicated that the oxidation of Al occurred at temperatures from 400 to 880 °C and sintering started at 1000 °C.

© 2003 Elsevier Ltd. All rights reserved.

*Keywords:* Al/ZrO<sub>2</sub>; Comminution; Milling; Oxidation; ZrO<sub>2</sub>

## 1. Introduction

Reaction bonding of aluminium oxide (RBAO) was developed to produce alumina based composites.<sup>1–4</sup> In this technique, attrition milled Al/Al<sub>2</sub>O<sub>3</sub> powder compacts are heat treated in air so that Al oxidises to ‘new’ Al<sub>2</sub>O<sub>3</sub> crystallites, which sinter and thereby bond together the originally added Al<sub>2</sub>O<sub>3</sub> or other ceramic particles. The main features of these composites are reduced shrinkage during processing and high strength of the product. The low shrinkage results from the partial compensation of the shrinkage due to sintering by an expansion associated with the oxidation of Al. The high strength is due to the fine grain size (< 1 μm) of Al<sub>2</sub>O<sub>3</sub> which develops during the RBAO process.

A combination of electrophoretic deposition (EPD) of YSZ/Al and the RBAO process has been used to produce ceramic coatings on metal substrates.<sup>5–7</sup> It has shown that the addition of aluminium to the green form composites not only led to the formation of crack-free composite coatings, but also promoted adhesion of ceramic coatings to metal substrate.<sup>5</sup> The RBAO process used in the above work was devised to overcome problems caused by the shrinkage during sintering, since

the 28% volume expansion associated with the Al→Al<sub>2</sub>O<sub>3</sub> reaction provided a compensating dimensional change.<sup>8</sup> However, the ball milling method used in the previous work limited the homogeneity of the coatings produced. No detailed study has addressed the properties of the YSZ/Al suspension. Water could be used as a solvent for suspension preparation since it has advantages of a high dielectric constant, low cost and less pollution. However, the electrolysis of water during EPD produced oxygen or hydrogen, which leads to formation of gas bubbles in the EPD deposit.<sup>9</sup> In addition, the milling of Al-ceramic in water led to extensive reaction between Al and water during milling.<sup>10</sup> Although there were extensive studies on milling of Al-ceramic suspension in organic solvents, e.g. acetone, 2-propanol, ethanol, etc.,<sup>11,12</sup> to our knowledge there is no study on attrition milling of YSZ/Al suspension in acetyl-acetone (ACAC).

In this study, attrition milling has been used to prepare metallic-ceramic suspensions. ACAC was used as a solvent because of its low volatilisation and low dielectric constant, which are desirable for the following EPD. Suspensions were characterised with particle size analyses and zeta-potential measurements. The powder was analysed using X-ray diffraction (XRD) and transmission electron microscope (TEM). The microstructures of the green coatings were examined using polarized optical microscope. Thermal analyses and

\* Corresponding author. Tel.: +44-161-200-5941; fax: +44-161-200-3586.

*E-mail address:* ping.xiao@man.ac.uk (P. Xiao).

dilatometry were used to study the oxidation of the Al and sintering of the coatings.

## 2. Experimental procedure

### 2.1. Suspension preparation

A mixture of 90 wt.% (80.5 vol.%) YSZ (HSY-8, Daiichi Kagaku Kogyo, Japan) and 10 wt.% (19.5 vol.%) Al powder (Alpoco, UK) was attrition-milled in acetyl-acetone (ACAC, Aldrich, UK). The attrition mill (type 01HD, Szegvari Attritor System, Union Process) with a 750ml-capacity milling tank, was loaded with 40 g of the powder mixture, 800g of tetragonal zirconia polycrystalline (TZP) milling balls (diameter of 3 mm), and 200 ml of ACAC. The rotation speed of the stirring arm of the attrition miller was 550 rpm while cooling water was used to keep the milling tank at a constant temperature. Suspensions were prepared with a dilution 10 times of the milling mixture with ACAC. The particle size distributions (PSD) and mean particle sizes in the suspensions were measured using a Mastersizer micro-plus (Malvern Ltd, UK). The zeta potential of the suspensions was examined using a DELSA 440 SX (Beckman Coulter, UK).

For thermal analyses, the milled powder–solvent mixture was separated from the TZP balls using a coarse sieve, and then dried on a hotplate at  $\sim 60$  °C. The dried powder was washed with ACAC five times in order to remove the organo-metallic compounds. The dried cake was ground using a mortar and pestle. The loose and dried powder was used for thermogravimetry/differential scanning calorimetry analysis (simultaneous TG/DSC Apparatus STA 449C Jupiter, Netzsch-Gerätebau GmbH, Postfach). The heating rate for thermal analysis is 3 degrees per minute from room temperature to 1200 °C, and remains at this temperature for 4 h. Phases and crystallites of the powders were identified using an X-ray diffraction technique (APD, Philips). The as-received YSZ powder and the milled YSZ powder were examined using a transmission electron microscope (CM200, Philips).

### 2.2. Electrophoretic deposition

Suspensions were prepared with a dilution 10 times of the milling mixture with ACAC. Before EPD, the suspension was subjected to ultrasonic vibration to break down weak agglomerates and to homogenize the suspension. EPD was performed by immersing two parallel electrodes (coating substrate as cathode and platinum electrode as anode) with a separation of 15 mm into the suspension. During EPD, the suspension was kept being stirred using a magnetic stirrer and a constant voltage of 80 V was applied between the two electrodes. After

deposition, green coatings were dried at room temperature. Microstructures of the green coatings were examined using polarized optical microscope.

## 3. Results and discussion

### 3.1. Influence of attrition milling on suspension

#### 3.1.1. Particle size distribution

In ceramic processing, milling has been used to reduce the particle sizes, to change the particle size distribution, to change the particle shape, to alter the surface activity and to disperse agglomerates.<sup>13,14</sup> However, milling has been mainly used to produce fine powder within a reasonable amount of time.<sup>12</sup> The attrition milling technique is more powerful than ball milling because the grinding energy can be increased significantly by increasing the rotation speed.

In this work, a mixture of YSZ (90 wt.%) and Al (10 wt.%) was attrition milled in ACAC. Fig. 1 shows the

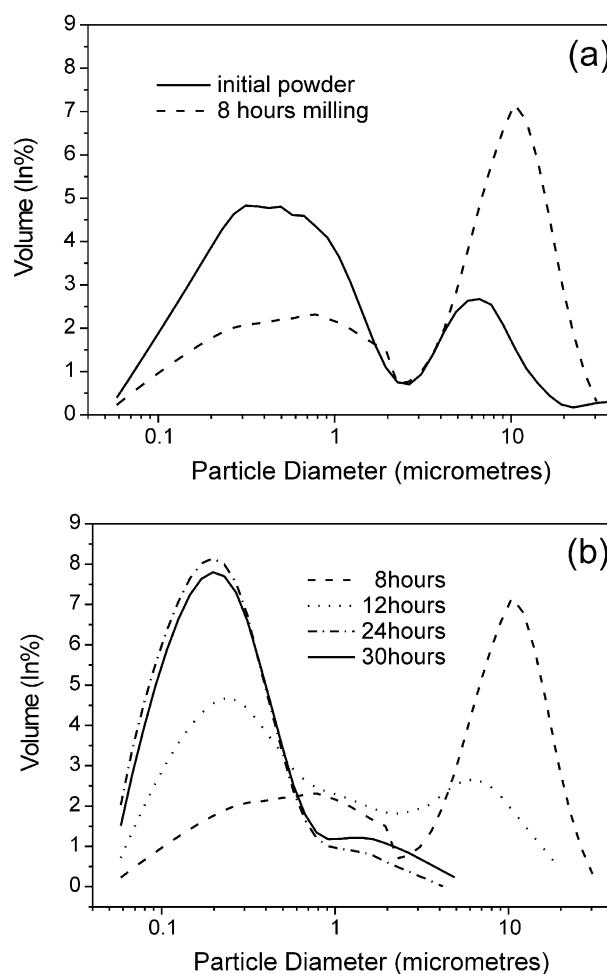


Fig. 1. Particle size distributions of powder mixtures a) as-received powder and after milling in ACAC for 8 h, (b) as a function of milling time in ACAC.

particle size distribution (PSD) of suspensions milled for different times. As shown in Fig. 1a, the initial powder has a bimodal distribution, which due to the presence of the two different powders, i.e., YSZ and Al. However, after 8 h milling, particle sizes for both the coarse particles and fine particles are larger than the initial particle sizes of the Al powder and YSZ powder, which were  $<6\ \mu\text{m}$  and  $\sim 0.3\ \mu\text{m}$ , respectively, as specified by the manufacturers and confirmed by particle size measurements before milling. Moreover, the volume percentage of the large particles ( $\sim 10\ \mu\text{m}$ ) in the suspension increased considerably to about 50 vol.%, while in the initial powder only 19.5 vol.% Al particles were added. In other words, the particle sizes in the suspension within the first 8 h milling increased rather than decreased. This unusual PSD change is due to a mechanical mixing between Al and YSZ particles. Similar phenomena were found by milling of oxide-Al particles in cyclohexane, leading to the formation of core/shell-like Al/oxide-particle agglomerates.<sup>15</sup>

Twelve hour milling considerably reduced the number of the large particles and increased the number of smaller particles (Fig. 1b). In the meantime, the average particle size of the small particles decreased from  $\sim 0.5\ \mu\text{m}$  for 8 h milling to  $\sim 0.2\ \mu\text{m}$  for 12 h milling. With a further increase in milling time, the large particles gradually diminished with a further increase in the number of the smaller particles. A nearly unimodal distribution was achieved after 24 h milling. The particle size decreased rapidly during the first 12 h milling, then decreased slowly. A milling time longer than 24 h did not seem to contribute to a further reduction of the particle size.

During attrition milling both shear and press forces acted on the particles by the milling media (i.e., TZP balls). Due to the malleability of Al, in the initial stage, Al particles could only be deformed and flattened by the milling forces, rather than be broken up immediately. At the same time, the hard and smaller YSZ particles were forced by the milling forces into the relatively soft Al particles to form a kind of mechanical mixture of Al with YSZ. This mechanical bonding action would make the large Al particles even larger and large particles increased their volume percentage in the suspension. This is the reason why the PSD of the suspension after 8 h milling shows a high percentage of large particles with a size larger than the original particles (Fig. 1a). As more YSZ particles penetrated into the Al particles, the ‘bonded’ particles became harder and less malleable and therefore they became more breakable. Large particles diminished with increase in milling time and the PSD tended to become unimodal.

It is difficult to distinguish Al and YSZ in the green coatings using SEM. This may be due to embedment of YSZ in Al. By using optical polarized illumination, the

Al appears brighter than the YSZ (Fig. 2). In the sample produced from 8 h milling there is a considerable amount of plate-type Al, which appear to be parallel to the substrate (Fig. 2a). It appears that some small YSZ particles are present in the Al plates. The increase in milling time eliminated almost all the large particles and Al particles were distributed uniformly throughout the green coating (Fig. 2b). This is in agreement with the results from the particle size measurements.

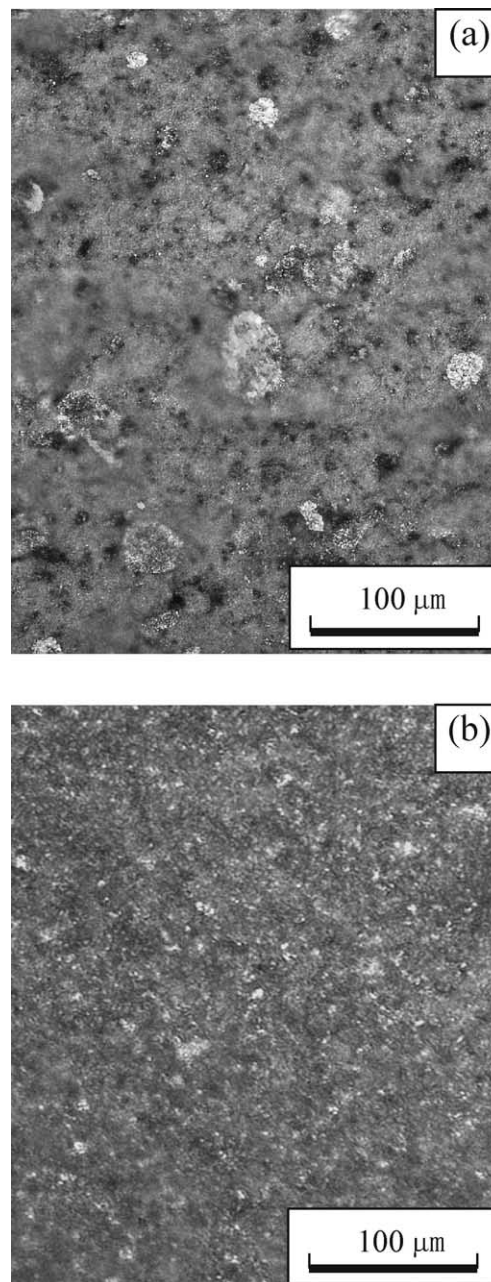


Fig. 2. Polarized optical images for coatings produced from suspension (a) milled for 8 h; (b) milled for 30 h. Al particles appear white while YSZ appear dark gray. Some YSZ particles are embedded in the Al particles.

### 3.1.2. YSZ Crystallites

ACAC is a beta-dicarbonyl compound. Due to the charge de-localisation over two oxygens, the central methylene group is strongly polarized. This means that ACAC is a polar solvent with a strong acidity. Fig. 3 shows XRD patterns of the particles from suspensions after attrition milling for different times. According to the XRD analyses,  $Zr(acac)_4$  and  $Al(acac)_3$  were formed during milling when ACAC reacted with both YSZ and Al. The XRD peaks of the organo-metallic compounds increased with increase in attrition milling time. In addition, the YSZ peaks become broader with increase in milling time. The half width of the (111) peak of YSZ is shown in Fig. 4a as a function of milling time. Peak broadening can be a result of either a distortion or a reduction in the size of the YSZ crystallites during milling. Assuming the peak broadening is mainly caused by a reduction of crystallite size, according to the Scherer equation,<sup>16</sup> the calculated crystallite size of the YSZ is from 60 nm before milling to 12 nm after milling for 24 h (Fig. 4b).

Figs. 5 and 6 show diffraction patterns and TEM images of the as-received YSZ powder and YSZ powder after attrition-milling in ACAC for 24 h. Both bright and dark images of the powder after milling (Figs. 6b and 6c) show the presence of smaller crystallites, in comparison to crystallites shown before milling (Fig. 5b). In addition, the ring-like diffraction pattern of Fig. 6a further suggests the crystallite size in the powder after milling is smaller than that in the as-received powder (Fig. 5a). Therefore attrition-milling did significantly reduce the crystallite size. Although it is difficult to give an accurate crystallite size of the YSZ before milling, according to Fig. 5b to the dark image of the YSZ after milling suggests that the crystallite size of the YSZ is between 10 and

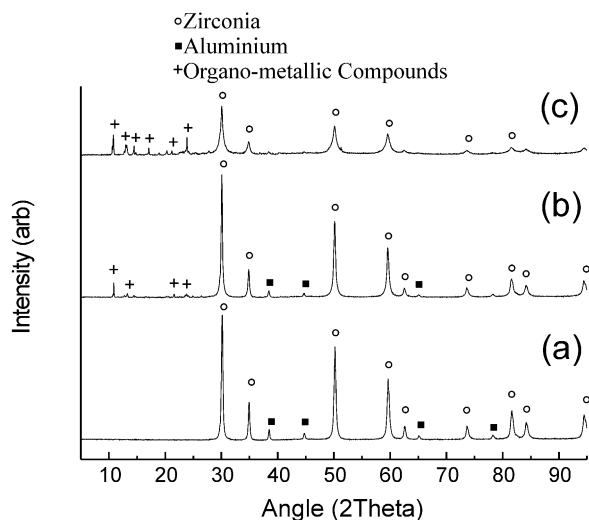


Fig. 3. XRD patterns of particles after attrition milling in ACAC, for (a) 4 h, (b) 12 h, and (c) 30 h.

20 nm. The change in YSZ crystallite size could be attributed to a chemical reaction between the YSZ and ACAC. Such reaction may occur preferably at grain boundaries in YSZ, therefore, reducing the grain size of YSZ. The mechanical forces applied during milling could promote this reaction.

### 3.1.3. Zeta potential

Fig. 7 shows the dependence of the zeta potential of the YSZ/Al suspension on the attrition milling time. The zeta potential increased with the attrition milling time, especially in the first 18 h. The zeta potential represents the formation of a double charge layer at the surface of particles, which controls the stability of the ceramic suspension and deposition direction. Electrostatic repulsive forces that are generated by common surface charges on the particles provide the main source of stabilisation of the suspensions. Two other effects, i.e., the steric hindrance and electrosteric repulsion may also promote stabilisation of suspension. A proper dispersion of a colloidal system in solvents is often

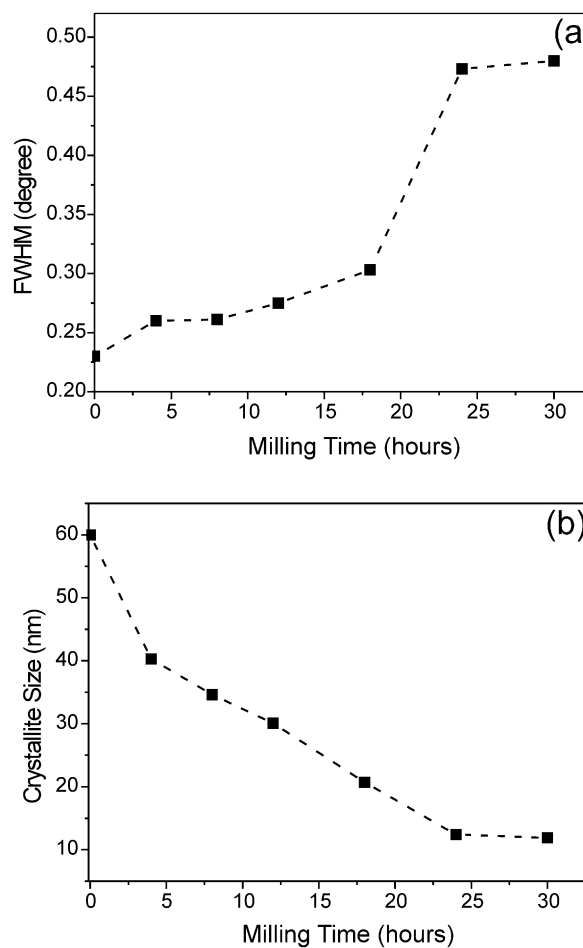


Fig. 4. (a) Half height width of the (111) peak in the XRD of YSZ, as a function of milling time; (b) calculated crystallite size of YSZ as a function of milling time.



achieved through control of the charge at the surface of particles by various means such as a change of pH, addition of charged poly-electrolytes or other potential-determining ions.

The chemical reactions between YSZ/Al and ACAC should release large amount of protons, according to Eqs. (1) and (2).<sup>17,18</sup> These free protons would be absorbed at the particle surface and subsequently YSZ and Al particles would be charged positively. As the milling time increased, more free protons would be produced and therefore particles would attract more protons, as a result of that, the zeta potential would increase.

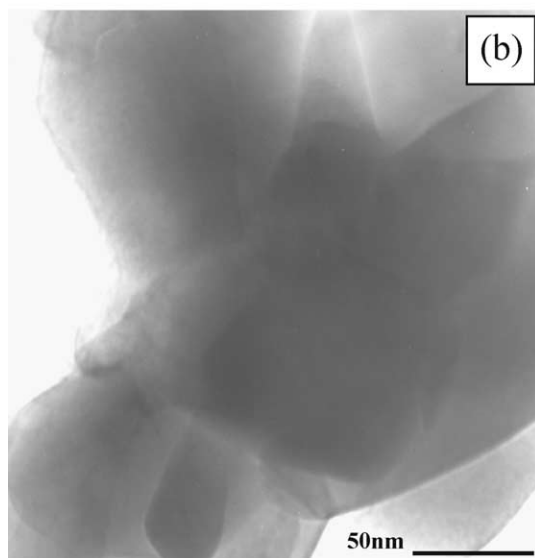
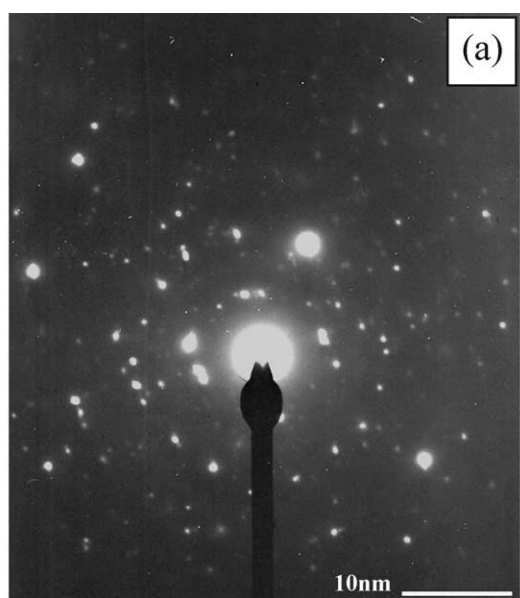
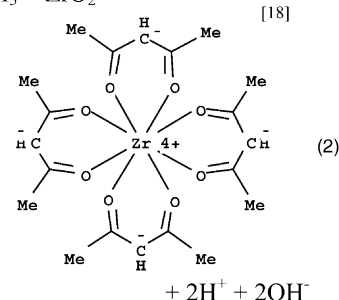
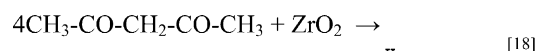
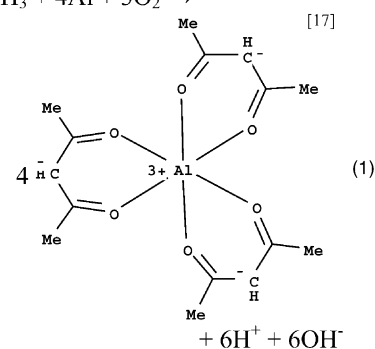
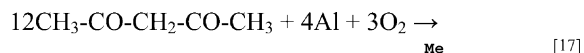


Fig. 5. (a) Diffraction pattern and (b) TEM image of the as-received YSZ particles.



### 3.2. Thermal analyses

The main purpose of adding aluminium into the green coating was to make use of the volume expansion due to the Al oxidation to compensate the shrinkage of the green coating during sintering. DSC analysis was used to characterize the oxidation/sintering process of YSZ/Al. The oxidation of aluminium is extremely exothermic ( $\Delta H = -1669.4 \text{ kJmol}^{-1}$ ) and is associated with a significant weight gain. To examine the effect of volume expansion due to the Al oxidation and shrinkage due to sintering, dilatometry analysis was carried out using a pure YSZ sample and a sample of the YSZ/Al mixture.

The dried power had been washed with ACAC several times in order to reduce the amount of the organometallic compounds before the TG/DSC and dilatometer analyses. Fig. 8 shows two exothermic peaks in the DSC plots. The first peak at 259.5 °C was accompanied by a weight loss that should be related to the oxidative decomposition of  $\text{Al}(\text{acac})_3$  and  $\text{Zr}(\text{acac})_4$  which were adsorbed on the particle surface. A significant weight gain from 400 to 590 °C corresponds to a sharp peak at  $\sim 537.4$  °C, indicating that the maximum Al oxidation rate occurs at  $\sim 537.4$  °C. This weight gain is believed to be due to the complete oxidation of small aluminium particles and the initial stages of oxidation of large Al particles. A slower weight gain between 590 and 880 °C may result from further oxidation of large aluminium particles, which occurred when the aluminium melted to allow the complete oxidation.

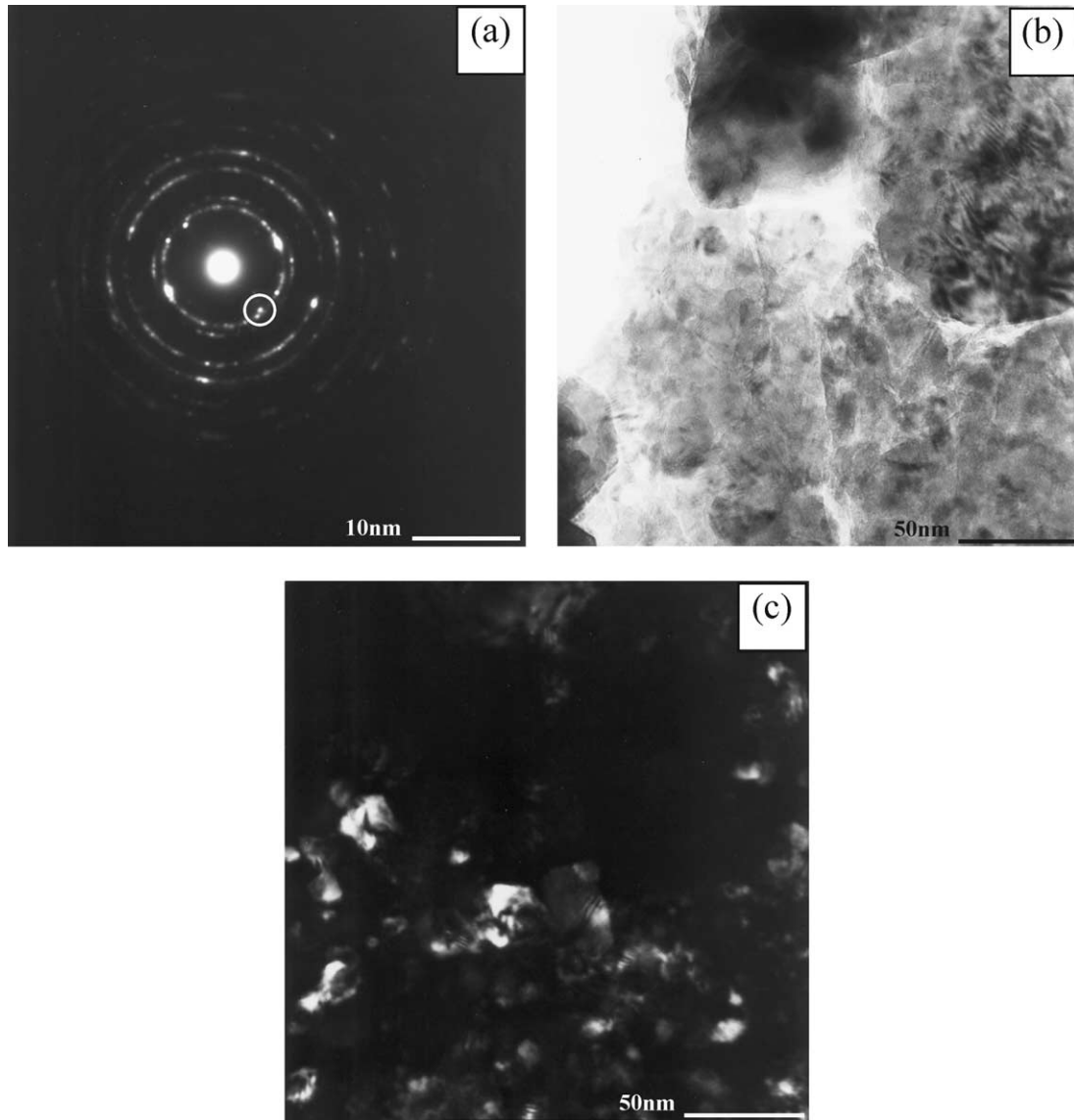


Fig. 6. (a) Diffraction pattern, (b) TEM bright image, (c) TEM dark image of YSZ powder after 24 h attrition milling in ACAC.

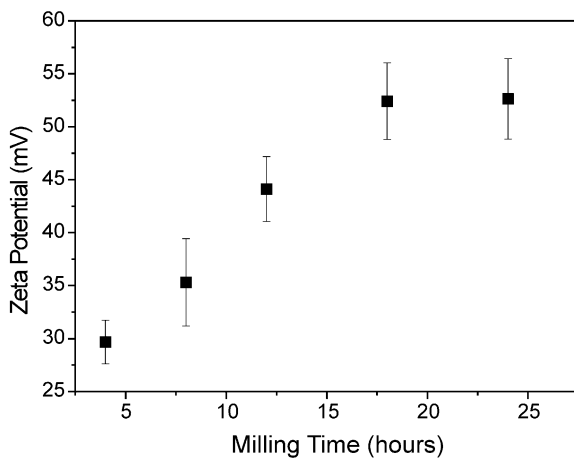


Fig. 7. Effect of attrition milling on zeta potential.

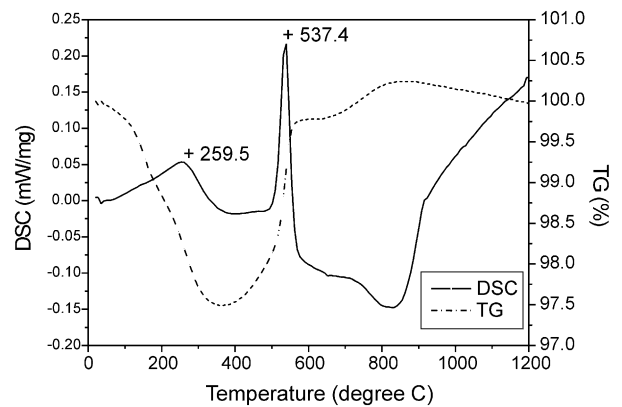


Fig. 8. TG/DSC result of YSZ/Al suspension milled for 24 h.

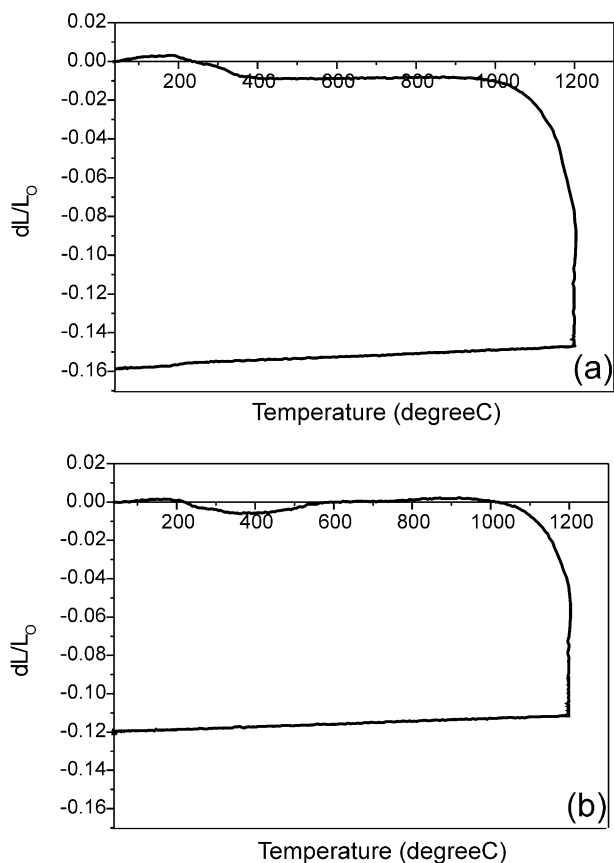


Fig. 9. Dilatometric curve of (a) a pure YSZ powder compact produced from the suspension attrition-milled for 24 h; (b) a YSZ/Al powder compact produced from a suspension attrition-milled for 24 h.

The aluminium oxidation examined here is similar to that studied previously on the RBAO, in which a similar oxidation temperature and DSC phenomena were reported.<sup>19</sup>

As shown in Fig. 9, both samples showed a shrinkage from 200 to 400 °C, which might be due to evaporation of  $Zr(acac)_4$  and  $Al(acac)_3$  adsorbed at the surface of the particles. The pure YSZ sample showed no expansion occurring from 400 to 1000 °C (Fig. 9a). In contrast, the YSZ/Al sample (Fig. 9b) showed a clear expansion from 400 to 600 °C, which can be attributed to the Al oxidation. The linear expansion due to oxidation is about 1%, which is much lower than the shrinkage (12–16%) due to sintering. Such expansion is associated with the oxidation of about 2.5 wt.% Al in the green compact, whereas 10 wt.% Al was added originally. Therefore, most of the Al was lost due to the chemical reaction between Al and ACAC, and the possible oxidation of Al by oxygen during milling. The addition of Al here has no significant effect on volume compensation. This is clearly in contrast with the RBAO process where the addition of Al was much higher (30–60 vol.%) and led to a significant expansion due to oxidation.<sup>1,10</sup> Furthermore, the sintering of  $Al_2O_3$  in the RBAO started

from 1200 °C, whereas sintering of YSZ/ $Al_2O_3$  in this study started at 1000 °C. Nevertheless, the addition of Al in this study promoted the adhesion of the coating to the metal substrate and hindered the formation of cracks in the coatings, in a similar way to the discovery in our previous work.<sup>5,6</sup> Further study is needed to understand the mechanisms controlling the coating/substrate bonding and crack formation.

#### 4. Conclusions

The attrition milling has a significant effect on the particle size distribution and grain size. As milling time increased, the particle size in the suspension changed gradually from a bimodal distribution to a nearly unimodal one. During attrition milling ACAC as solvent reacted with both YSZ and Al particles. The chemical reactions might lead to a reduction of crystallite size of YSZ. The zeta potential of the suspension was found to increase with the milling time, which might also be due to the chemical reaction between ACAC and solid particles. Thermal analyses indicated that Al particles were oxidised at about 540 °C, and sintering started at 1000 °C. The volume expansion due to the Al oxidation was insignificant in comparison with volume shrinkage due to sintering.

#### References

1. Claussen, N., Wu, S. and Holz, D., Reaction bonding of aluminium oxide (RBAO) composites: processing, reaction mechanisms and properties. *J. Eur. Ceram. Soc.*, 1994, **14**, 97–109.
2. Claussen, N., Janssen, R. and Holz, D., Reaction bonding of aluminium oxide (RBAO). *J. Ceram. Soc. Jpn.*, 1995, **103**(8), 749–758.
3. Garcia, D. E., Janssen, R. and Claussen, N., Microstructure development in in situ reinforced reaction-bonded aluminium niobate-based composites. *J. Am. Ceram. Soc.*, 1996, **79**(9), 2266–2270.
4. Gaus, S. P., Chan, H. M., Harmer, M. P. and Caram, H. S., Macroscopic modelling of the reaction bonding of aluminium oxide. *J. Eur. Ceram. Soc.*, 1997, **17**, 971–975.
5. Wang, Z., Shemilt, J. and Xiao, P., Fabrication of ceramic composite coatings using electrophoretic deposition, reaction bonding and low temperature sintering. *J. Eur. Ceram. Soc.*, 2002, **22**, 183–189.
6. Wang, Z., Xiao, P. and Shemilt, J., Fabrication of composite coatings using a combination of electrochemical methods and reaction bonding process. *J. Eur. Ceram. Soc.*, 2000, **20**, 1469–1473.
7. Wang, Z., Shemilt, J. and Xiao, P., Novel fabrication technique for the production of ceramic/ceramic and metal/ceramic composite coatings. *Scripta Mater.*, 2000, **42**, 653–659.
8. Claussen, N., Le, T. and Wu, S., Low shrinkage reaction bonded alumina. *J. Eur. Ceram. Soc.*, 1989, **5**, 29–35.
9. Heavens, S. N., Electrophoretic deposition as a processing route for ceramics. In *Advanced Ceramic Processing and Technology, Vol. 1*, ed. Jon G.P. Binner. Noyes Publications, Park Ridge, NJ, 1990, pp. 264–266.

10. Holz, D., Wu, S., Scheppokat, S. and Claussen, N., Effect of processing parameters on phase and microstructure evolution in RBAO ceramics. *J. Am. Ceram. Soc.*, 1994, **77**(10), 2509–2517.
11. Suvaci, E., Simkovich, G. and Messing, G. L., The reaction-bonded aluminium oxide process I: the effect of attrition milling on the solid-state oxidation of aluminium powder. *J. Am. Ceram. Soc.*, 2000, **83**(2), 299–305.
12. Watson, M. J., Chan, H. M., Harmer, M. P. and Caram, H. S., Effects of milling liquid on the reaction-bonded aluminum oxide process. *J. Am. Ceram. Soc.*, 1998, **81**(8), 2053–2060.
13. Kelly, E. G. and Spottiswood, D. J., *Introduction to Mineral Processing*. Wiley, New York, 1982.
14. Summers, W., Broad scope particle size reduction by means of vibratory grinding. *J. Am. Ceram. Soc. Bull.*, 1983, **62**(2), 212–215.
15. Essl, F., Bruhn, J., Janssen, R. and Claussen, N., Wet milling of Al-containing powder mixtures as precursor materials for reaction bonding of alumina (RBAO) and reaction sintering of alumina-aluminide alloy (3A). *Materials Chemistry and Physics*, 1999, **61**, 69–77.
16. Cullity, B. D., Structure of polycrystalline aggregates, In *Elements of X-ray Diffraction*, 1978, 2nd ed. p 284 Addison–Wesley Publishing Company, Inc.
17. Hon, P. K. and Pfluger, C. E., Crystal and molecular structure of tris(acetylacetonato)aluminum(III) and-cobalt(III). *J. Coord. Chem.*, 1973, **3**(1), 67–76.
18. Ezhov, Yu.S., Komarov, S. A., Sevast'yanov, V. G., Timofeev, A. N. and Filatov, I.Yu., Structure of the molecule of zirconium acetylacetonate. *Nauchno-Issled. Inst. Khim. Reakt. Osobo Chist. Khim. Veshchestv, Moscow, Russia, Vysokochistye Veshchestva*, 1995, **1**, 89–95.
19. Wu, S., Holz, D. and Claussen, N., Mechanisms and kinetics of reaction-bonded aluminium-oxide ceramics. *J. Am. Ceram. Soc.*, 1993, **76**, 970–980.